

### **MALAYSIAN JOURNAL OF ANALYTICAL SCIENCES**



Journal homepage: https://mjas.analis.com.my/

# **Research Article**

# Magnetic bead catalyst for photocatalytic phenol degradation in wastewater

Diyana Faziha Mohamad<sup>1</sup>, Muhammad Farhan Hanafi<sup>1</sup>, Norezatul Shahirah Ahmad Zamanhuri<sup>1</sup>, Siti Kamilah Che Soh<sup>2</sup>, Cecilia Devi Wilfred<sup>3</sup>, Dayang Norafizan Awang Chee<sup>4</sup>, Haniza Kahar<sup>1,\*</sup>, and Norzahir Sapawe<sup>1,\*</sup>

<sup>1</sup>Universiti Kuala Lumpur, Branch Campus Malaysian Institute of Chemical and Bioengineering Technology (UniKL MICET), Lot 1988 Vendor City, Alor Gajah, Melaka, Malaysia

<sup>2</sup>Faculty of Science and Marine Environment, Universiti Malaysia Terengganu (UMT), 21030 Kuala Terengganu, Terengganu, Malaysia

<sup>3</sup>Department of Fundamental and Applied Sciences, Universiti Teknologi PETRONAS (UTP), 32610 Seri Iskandar, Perak, Malaysia

<sup>4</sup>Faculty of Resource Science and Technology, Universiti Malaysia Sarawak (UNIMAS), 94300 Samarahan, Sarawak, Malaysia

Received: 7 October 2024; Revised: 20 April 2025; Accepted: 21 May 2025; Published: 15 June 2025

#### Abstract

Modern advances in semiconductor photocatalysis, particularly increased turnover on degradation of phenolic compounds from industrial wastewater. Phenolic compound is a major environmental threat considering their hazardous effects and recalcitrance. This study focused on the development of high efficiency magnetic bead catalyst with photocatalysis technology as a solution to phenolic compound obstacles in industrial wastewater. The magnetic bead catalyst underwent bead casting process by encapsulating a polymer matrix of sodium alginate and crosslinking it with epichlorohydrin, which enhancing its hydrophilicity, durability, rigidity, selectivity, permeability, and longevity, thereby achieving superior photocatalytic performance. Characterisation techniques including Fourier-transform infrared spectroscopy (FTIR) and X-ray diffraction (XRD) were employed to analyse the structural and chemical properties of these catalyst. The photocatalytic efficiency of the magnetic bead catalyst for the degradation of phenol was assessed when subjected to visible light. A comprehensive study was conducted exploring the effects of pH, catalyst dosage, and initial phenol concentration on effectiveness of degradation. The optimal conditions for the Fe-beads catalyst were achieved at pH 5, with a dosage of 6.0 g L<sup>-1</sup> and an initial phenol concentration of 20 mg L<sup>-1</sup>, resulting in a phenol photodegradation efficiency of 87.29%. These magnetic bead catalyst implementations for wastewater recovery were cost-effective, quick to implement, eco-friendly, and regenerable. In short, synthesising magnetic bead catalyst might pose an innovative approach towards challenges with wastewater treatment.

Keywords: magnetic beads catalyst, phenol, photocatalytic degradation, visible light irradiation, wastewater treatment

## Introduction

Water, the essence of life, is the cornerstone of Earth's ecosystems. However, the world's finite freshwater resources are increasingly threatened by pollution from the continuous discharge of untreated or poorly treated wastewater into reservoirs, lakes, rivers, and coastal regions. This escalating contamination poses a severe risk to public health, with over one-third of the global population lacking access to clean water and proper sanitation [1]. Untreated industrial effluents released into water bodies not only jeopardise human health but also inflict substantial environmental

damage. The World Health Organisation (WHO) warns that water pollution currently affects millions worldwide, with projections indicating that this crisis could impact 3.7 billion people by 2025 [2]. Phenolic compounds are identified as a major contributor to water pollution, presenting significant environmental and health challenges due to their persistence in the environment, ability to accumulate over time, and detrimental effects on various organisms. The U.S. Environmental Protection Agency (USEPA) identifies phenol as one of the most hazardous chemicals [3]. Phenolic compounds are extensively utilised in

<sup>\*</sup>Corresponding author: norzahir@unikl.edu.my, hanizakahar@unikl.edu.my

industries, such as paper manufacturing, plastics, pesticides, petrochemicals, and pharmaceuticals. These industries discharge substantial quantities of waste containing phenol into the environment, often with concentrations far exceeding normal water levels—sometimes in the range of millions of milligrams per litre [4].

Phenolic compounds can undergo transformations physical, chemical, biological, microbiological interactions, leading to the formation of potentially more toxic substances upon entering aquatic systems. Excessive phenol exposure in humans can harm several organs, including the digestive system, eyes, respiratory system, cardiovascular system, brain, and skin. In industrial effluents, phenol concentrations typically range from 10 mg L<sup>-1</sup> to 300 mg L<sup>-1</sup>, with highly contaminated effluents reaching up to 4.5 g L<sup>-1</sup>. Moreover, chlorinating phenol-laden water for disinfection can result in the formation of harmful polychlorinated phenols. At concentrations between 5 mg L<sup>-1</sup> and 25 mg L<sup>-1</sup>, phenol and its derivatives are toxic or lethal to fish and may also exhibit carcinogenic properties. Even at lower concentrations (2 g L<sup>-1</sup>), phenol imparts an unpleasant medicinal taste and odour to water. According to the World Health Organisation (WHO), the maximum safe phenol concentration in drinking water is 1 g  $L^{-1}$  [5].

A variety of technology-driven solutions are being explored today to address these environmental challenges. The rapid growth of technology over the past few decades, one of the main areas of concern in modern times is the search and utilisation of renewable energies. The renewable nature, ease of use, and mobility of solar energy have made it a highly regarded choice for sustainable technology [6] such as photocatalysis. The photocatalysis is a unique technique that is widely used in many interdisciplinary study disciplines. These days, photocatalysis shows great promise for recovering ecological principles and advances in sustainability. Since the process can be influenced by light or photon sources, photocatalysis theoretically requires radiation to activate electrons to shift to begin the reaction. These processes produce highly reactive species, such as hydroxyl radicals (•OH), which can engage with various organic compounds via electrophilic addition to double bonds or electron-transfer reactions. The intermediates formed can subsequently react with dissolved molecular oxygen, boosting degradation efficiency and transforming contaminants into less harmful or non-toxic substances [7-13].

In photocatalysis, magnetite and maghemite are both often used [14]. Iron oxide nanoparticles clump together because of their high surface to volume ratio,

demonstrating an important proportion of surface energy. Amongst the several forms of iron oxide that are known to exist are haematite (Fe<sub>2</sub>O<sub>3</sub>), maghemite (Fe<sub>2</sub>O<sub>3</sub>), and magnetite (Fe<sub>3</sub>O<sub>4</sub>). Iron oxide nanoparticles' dispensability and magnetic function are diminished by their strong reactivity, leading to oxidised them promptly the environment. Therefore, it is imperative to maintain the iron oxide equilibrium, and this is easily achieved by carefully encapsulating the nanoparticles with organic ligands, polymers, and monomers [15]. Deposition of Fe<sub>3</sub>O<sub>4</sub> nanoparticles lowers surfaceactive regions, a feature essential for improved diffraction of light. The photocatalysts may be easily retrieved from the method of processing in the aid of a magnetic external field, catalysts that integrate with magnetism catalytic properties allow photocatalysts to be regenerative. The enhanced optical, chemical-based magnetic, electrical, and thermal stability of magnetic iron oxide nanoparticles has allowed them to be used in a variety of applications, such as dyes, data storage, electronic products, catalysis, ferrofluids, and medical treatments [16].

The optimal photocatalytic degradation can be achieved in this study by incorporation of magnetic nanoparticles with sodium alginate. This integration boosts the material's surface area, improving its attraction to hydroxyl groups and promoting the formation of hydroxyl radicals. Sodium alginate, an anionic polysaccharide, has gained popularity as a polymeric adsorbent due to its long shelf life, costeffectiveness, adsorption-regeneration and capabilities. Composed of β-D-mannuronic acid and α-L-guluronic acid, sodium alginate can be formed into hydrogel beads and chemically modified through cross-linking of its α-L-guluronic acid units with polyor divalent cations [17]. Widely utilised as a support framework for polymeric catalysts, alginate offers numerous advantages as a bio sorbent. Its hydrophilic nature, natural abundance, active binding sites, and sustainability contribute to its superior performance. The carboxylate structure provides additional active sites for adsorption and catalysis. Moreover, surfacebound inorganic or organic shells stabilise and prevent the oxidation of metal oxide nanoparticles. Encasing the magnetic nanoparticle catalyst in sodium alginate enhances its hydrophilicity, making it a versatile and efficient component for photocatalytic applications.

The addition of support materials, which is alginate has gained significant attention due to its potential to enhance photoactivity, driven by the synergistic effect between the metal oxide and the support material. Magnetic beads combined with alginate were selected for their ability to enhance photocatalytic performance in several keyways. First, alginate serves as an

excellent stabiliser, preventing the aggregation of magnetic particles and improving the stability and durability of the catalyst. This ensures more consistent performance over time, which is often a challenge with bare magnetic beads. Additionally, the magnetic beads allow for easy recovery using an external magnetic field, making them highly recyclable. The alginate coating helps protect the beads from degradation during repeated cycles, addressing the common issue of catalyst loss seen with other materials like TiO2 or ZnO. This contributes to the cost-effectiveness of the system. The synergistic effect of the magnetic beads and alginate further improves photocatalytic performance. The alginate matrix contains functional groups such as hydroxyl or carboxyl groups, which can interact with and adsorb pollutants, increasing their concentration at the catalyst's active sites. This interaction enhances the efficiency of the photocatalytic process. Moreover, alginate is biodegradable and environmentally friendly, making it a more sustainable option compared to non-biodegradable catalysts like TiO2 or ZnO.

Overall, the combination of magnetic beads and alginate is expected to provide superior photocatalytic performance by offering improved stability, recyclability, and cost-effectiveness, while also being environmentally friendly. These attributes make magnetic beads a promising alternative in catalytic applications, offering both practical and economic benefits. Current work on the advancement of magnetic bead catalysts and nanomaterials holds great promise, especially for purifying water processes. Given its porous architecture and greater surface area, the nanoparticles in magnetic bead catalyst possess the ability to respond swiftly. They may further be functionalised with various chemical groups to boost their selectivity or reactivity for a specific molecule. The process for developing magnetic strengthened the shape and arrangement of the iron particles, resulting in turn boosted the catalyst's capabilities and accelerated the breakdown of phenol in water. These findings have led to an interest in exploring the synthesis of Fe<sub>3</sub>O<sub>4</sub> supported on polymer matrix of and Fourier transform infrared (FT-IR). The activity of the catalyst for the photodegradation of phenol was studied under various conditions to determine the effect of pH, catalyst dosage, and initial phenol concentration.

## Materials and Methods Chemicals and Materials

All chemicals were brought in analytical grade and used without further purification. Iron (II, III) oxide magnetic (Fe<sub>3</sub>O<sub>4</sub>) was obtained from Bendosen Laboratory Chemicals, ethanol absolute (C<sub>2</sub>H<sub>5</sub>OH) (> 99% purity) from HmbG Chemicals, calcium chloride

(CaCl<sub>2</sub>) was obtained from R&M Chemicals and sodium hydroxide (NaOH), hydrochloric acid (HCl), were obtained from QReC<sup>TM</sup>. Glutaraldehyde (25% (v/v)) solution (C<sub>5</sub>H<sub>8</sub>O<sub>2</sub>), phenol (C<sub>6</sub>H<sub>5</sub>OH) and sodium alginate (NaC<sub>6</sub>H<sub>7</sub>O<sub>6</sub>) were purchased from Sigma-Aldrich (Malaysia).

#### **Preparation of samples**

The precursor solution was prepared by dissolving the powdered catalyst in 3% wt. of alginate solution which prepared by deionised water to form a viscous solution and well-mixed. The prepared solution is then pumped by using a syringe into a precipitation bath (non-solvent) that consists of 0.5M aqueous CaCl<sub>2</sub>. The wet beads formed then cross-linked with epichlorohydrin solution and the reaction take place at room temperature. Initially, magnetic zeolite bead catalyst was immersed in three successive ethanol/water baths (60% v/v ethanol, 400 mL each) for 2 h each to replace the water in the beads with ethanol. The beads were then transferred to 400 mL of an ethanol/water solution (60% v/v ethanol) containing epichlorohydrin (6.109 g). A 1 mol/L NaOH solution was gradually added to adjust the pH to approximately 13. The crosslinking reaction was carried out for 4 h. The beads were rinsed subsequently in three consecutive baths of distilled water (600 mL each for 2 h). In the final bath, concentrated HNO<sub>3</sub> solution (53.7% w/w) was added to neutralise the mixture, bringing the pH to around 7. The final step of bead fabrication is freeze-dried for removing the excess water in the pore structure.

# Material characterisation of samples

Absorption spectra of the samples were recorded by using Nicolet iS10 FTIR spectrophotometer with wavenumber range from 4,000 cm<sup>-1</sup> to 400 cm<sup>-1</sup> to study the chemical bonding of the mixture in the sample. The powdered tablet samples were placed on Smart iTR<sup>TM</sup> Attenuated Total Reflectance (ATR) accessory composed of diamond crystal as sample handling technique at a controlled ambient temperature (25°C). The samples were scanned by using Nicolet iS10 FTIR spectrophotometer (Thermo Fisher Scientific Inc, Madison, USA) equipped with deuterated triglycine sulphate (DTGS) detector and potassium bromide (KBr) as a beam splitter. The air spectrum was used as background.

The XRD spectra analysis was performed by D8 ADVANCE Bruker X-ray diffractometer using Copper K- $\alpha$  radiation source at a  $2\theta$  angle of  $10^{\circ}$  to  $90^{\circ}$  with a step size of 0.02 with Xpert Pro X-Ray Diffraction System at ambient temperature. XRD analysis was run to determine the materials crystalline phase and crystalline particles sizes for each sample. The phases are assessed by evaluating the gathered information data from prior studies data bases. The

Debye-Scherrer equation was used to compute the crystalline particle sizes of the bead catalysts phases.

## Photocatalytic performance study

photocatalytic degradation of phenolic contaminants has been utilised to assess the photocatalytic activity of the magnetic bead catalyst. research's photocatalytic reactions conducted in the presence of visible light. The study examined the influence of various factors, including solution pH (3, 5, 7, 9, 11), bead catalyst dosage (2.0,  $4.0, 6.0, 8.0, 100.0 \text{ g L}^{-1}$ ), and initial concentrations of phenol (20, 40, 60, 80, 100 mg L<sup>-1</sup>). These experiments were conducted under visible light for 2 h with continuous stirring, using a magnetic bead catalyst. To get the appropriate pH, 0.1 M NaOH or/and 0.1 M HCl solution was added to the sample mixture. Approximately 2.0 g L-1 (wet weight) of bead was poured into a beaker with 100 mL of sample solution (20 mg L<sup>-1</sup>). A magnetic stirrer was used to gently swirl the liquid continuously for 120 min. The sample solution was subjected to an irradiation source, a fluorescent light, with a 15 cm height restriction separating the solution and the illumination source. Each sample was measured with 1.5 mL using a Shimadzu UV-2600i UV-vis spectrophotometer at a predetermined interval of contact (0, 30, 60, 90, and 120 min) and the phenol concentration was assessed at the specified wavelength of 293 nm.

#### **Results and Discussion**

## Characterisation of magnetic bead catalyst

Studies via infrared spectra was conducted to evaluate the catalyst's chemistry and impurity of the beads. Atomic vibrations in metal oxides often result in significant absorption peaks in the fingerprint area with values less than 1,000 cm<sup>-1</sup>. In order to ascertain the functional existence and enquire into the chemical relationships of the accomplish composition in the material under study Fe-bead catalyst and Alginate beads the FTIR spectrum was measured at wavelengths between 4,000 cm<sup>-1</sup> - 400 cm<sup>-1</sup>. **Figure 1** shows the FTIR spectra of the alginate beads and the generated Fe-beads catalyst.

A noticeable and broad band at 3,446.96 cm<sup>-1</sup>, which corresponds to the presence of OH hydroxyl group in the Fe-beads catalyst sample. This was due to H<sub>2</sub>O molecules adsorbed on catalyst surface, and visible in the FTIR spectrum that the catalyst exhibited and is shown in **Figure 1**. The peak vibrations at 2,368.26 cm<sup>-1</sup> arise in the interim because of the carbon triple bond (−C≡C−) triple bond deformation. It has been discovered that the COO⁻ of alginate produced the two distinct bands at 1,638.11 cm<sup>-1</sup> and 1,413.43 cm<sup>-1</sup>, corresponding to symmetric and asymmetric stretching vibrations, correspondingly. The peaks determined Fe-beads catalyst was functionalised with

carboxyl groups (-COOH), corresponding to the C=O stretching vibration from alginate-beads. The spectral band at 1,121.15 cm<sup>-1</sup> seems to be responsible for the symmetric C-O vibration. The Fe-O stretching band of bulk magnetite Fe<sub>3</sub>O<sub>4</sub> nanoparticles is roughly correlated to substantial spectrum of absorption at widths of about 570.36 cm<sup>-1</sup>. The absorbance bands with centring spans of 760 cm<sup>-1</sup> to 500 cm<sup>-1</sup> have been identified to reflect the Fe<sup>2+</sup>-O-Fe<sup>3+</sup>, Fe<sup>3+</sup>-O, and Fe<sup>2+</sup>-O bonds from Fe<sub>3</sub>O<sub>4</sub> [18]. These results support the XRD analysis data, which is indicative of the purity of the Fe-beads catalyst sample.

The FTIR spectrum of the alginate-beads, as shown in Figure 1, suggested that C-H stretching was responsible for the range of the absorbed band of sodium alginate seen at 2,957.24 cm<sup>-1</sup>. However, no obvious band was observed in this region on Fe-beads catalyst surface. It may be because of overlapping with magnetic material characteristic stretching frequencies in this region. In this region, the peak indicated Fe-beads catalyst was coated with polymers coating, which is sodium alginate from alkyl groups in this region. The existence of vibrations linked to alginate's O-H bond stretching in the range of 3,000 cm<sup>-1</sup> to 3,600 cm<sup>-1</sup> is indicated by the strong band at 3,448.13 cm<sup>-1</sup> on alginate-beads surface, which involved in hydrogen bonding. The peak at 2,368.22 cm<sup>-1</sup> is the output of the carbon triple bond's triplebonded stretching vibration (−C≡C−). The asymmetric vibrations of carboxylate salt ions were also responsible for the bands seen at 1,636.83 cm<sup>-1</sup> and 1,389.10 cm<sup>-1</sup>, respectively. The band seen at 1,122 cm<sup>-1</sup> was associated with the C-O-C deformation of ethers. A significant changing in the intensity of these peaks were observed after Fe<sub>3</sub>O<sub>4</sub> loading, which suggested a possible interrelationship of Fe<sub>3</sub>O<sub>4</sub> on the -COOH. This result suggests that Fe<sub>3</sub>O<sub>4</sub> may be inserted into the sodium alginate framework.

The XRD analysis relies on Bragg's equation  $n\lambda = 2d \sin \theta$ , where n represents the order of diffraction,  $\lambda$  represents the incident X-ray wavelength (Cu, 0.15406 nm), d represents the interplanar spacing (hkl), and  $\theta$  represents the angle that exists amongst the incident X-ray and the scattering planes. The XRD spectra was performed by using Copper K- $\alpha$  radiation source at a 2 $\theta$  angle of 10° to 90° with a step size of 0.02 at room temperature. Figure 2 displays the diffractogram outcomes of the Fe-bead catalyst sample data.

The diffractogram of Fe-beads catalyst was demonstrated the diffraction peaks 2θ appearing in the XRD pattern around 19.29°, 30.43°, 35.83°, 43.39°, 57.35°, and 62.9° corresponding to the planes with Miller indices (110), (220), (311), (400), (511) and

(440), respectively (**Figure 2**), which is consistent with the referenced data for maghemite (Fe<sub>3</sub>O<sub>4</sub> nanoparticle) (JCPDS file no. 19-629). The XRD of the synthesised bead revealed peaks corresponding to pure crystallites of magnetite (JCPDS file no. 19-629) with no impurities where no other phase of Fe(OH)<sub>3</sub> or Fe<sub>2</sub>O<sub>3</sub> was detected. The previously described peaks' distribution indicates that Fe<sub>3</sub>O<sub>4</sub> has a crystalline framework with a spinel configuration. Debye-Scherrer equation was adopted to calculate the average crystallite size of the Fe-beads catalyst based on the principal peak at 35.83° (311), measured at

28.77 nm. Intense peaks indicate the sample had excellent crystallinity, whereas wide peaks suggest that the Fe-beads catalyst sample was manometer-sized. Since the crystal dimension is getting closer to the nanoscale, it has been observed that the peak expands with decreasing crystal size. These results showed that the Fe<sub>3</sub>O<sub>4</sub> nanoparticles were highly pure and had excellent crystallinity, and they were in perfect accord with previous data published in research [18].

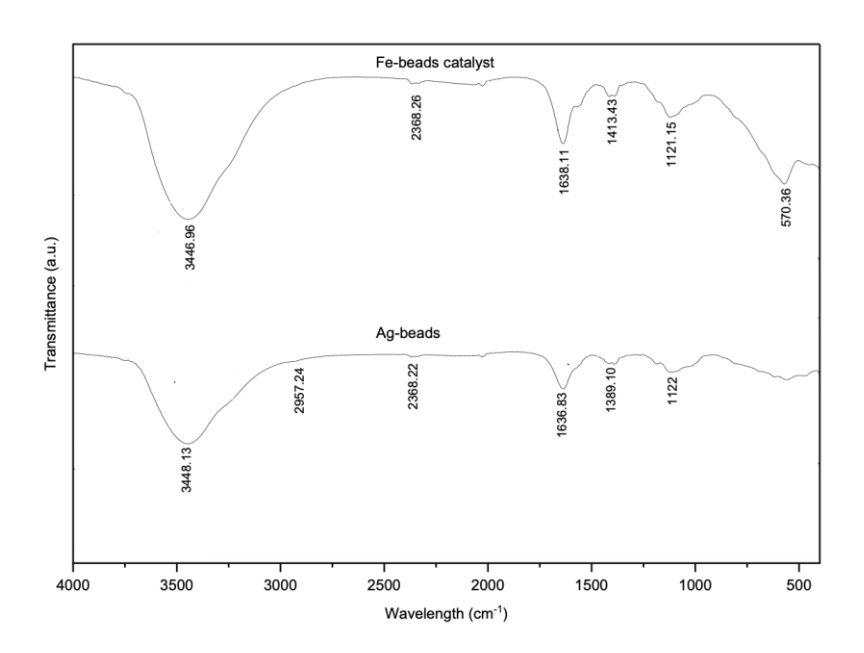


Figure 1. FTIR spectra for Fe-beads catalyst and Alginate-beads

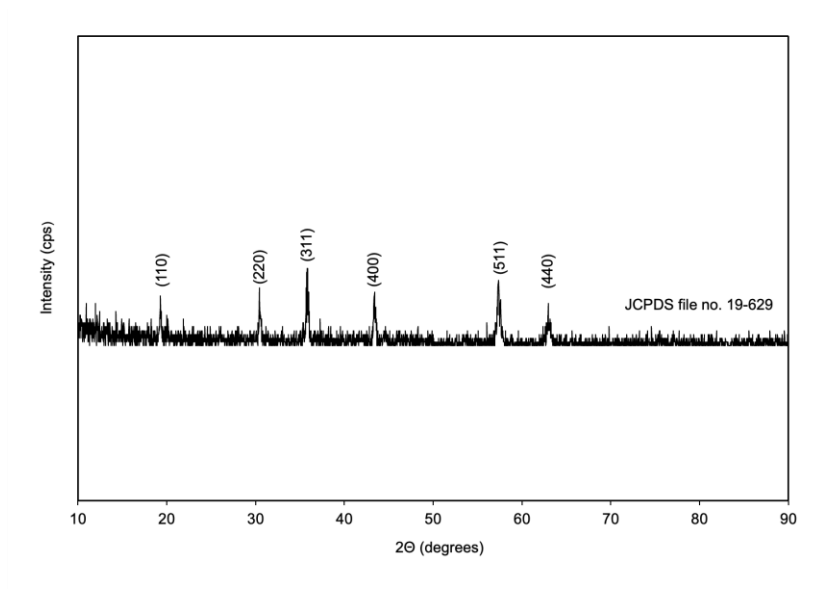


Figure 2. XRD phase of Fe-beads catalyst

## Photocatalytic performance studies

The photodegradation of phenol in a water-based solution was implemented to assess the photodegradation activity of the produced beads catalyst. The effect of the pH solution, the dosage of the catalyst, and the initial pollutant concentration were the parameters that underwent assessment to evaluate the degradation activity. The investigations on batch sorption were carried out at the ambient temperature over a two-hour duration of contact.

The pH of the solution has a major impact on how rapidly pollutants degrade by photodegradation. Typically, semiconductor oxides exhibit amphoteric behaviour, which mostly impacts the surface-charge properties of photocatalysts since responses occur on the semiconductor's active site surface. The highest rate of phenol degradation for Fe-beads catalyst was seen in the present research at pH 5 (Figure 3). At pH 5, the highest degradation rate of 69.60% of photodegradation rate phenol was attained. The outcomes were consistent with the pH investigation conducted by Ahmad et al. [19], which demonstrated that the degradation rate decreased as pH increased from 5 to 11. A higher generation of HO• at more acidic to medium pH values accounts for the improvement in performance at pH 5. As pH increased, oxyhydroxides such Fe(OH) and FeOH+ were produced, which had previously adsorbed at the surface of the Fe-beads catalyst. This resulted in a progressive decrease in the efficacy of degradation. The significant decrease in performance at pH 11 was attributed to the reduced capacity of HO• oxidation, which results in the production of inactive ferrous ions (FeO<sup>2+</sup>) at elevated pH levels [20]. The dissociation of hydrogen peroxide in alkaline settings explains the following. Hydrogen peroxide and hydroxyl radicals break down quickly at elevated pH levels.

The following was supported by more favourable interactions at lower pH levels, compared to the interactions between pollutant molecules and the Febeads catalyst at acidic to neutral pH. This is attributed to the Fe-beads catalyst having a point of zero charge (pH<sub>pzc</sub>) of 5.1. At pH<sub>pzc</sub> = 0, the catalyst surface would be neutral, at pH<sub>pzc</sub> > 5.1, it would be negatively charged, and at pH<sub>pzc</sub> < 5.1, it would be positively charged. At higher pH, the negatively charged Febeads catalyst surface repels the anionic phenol molecules due to electrostatic forces. In contrast, at pH 3 (acidic conditions), excess H<sup>+</sup> ions in the phenol

solution can protonate the catalyst surface, resulting in a positively charged surface that limits the availability of active sites on the catalyst for phenol photodegradation.

Another crucial step in the photocatalytic process is determining the ideal catalyst dosage for maximum efficiency. Figure 4 illustrates the assessment effect Fe-bead catalyst dosage on photodegradation. It shows that photodegradation of phenol increased dramatically with increasing Febead catalyst dosage, until it plateaued at a specific threshold. At a dose of 6.0 g L<sup>-1</sup>, the Fe-bead catalyst's maximum photodegradation rate was 87.19%. Whenever the total quantity of bead catalyst is increased in response to the situation at this moment the photocatalytic reactions created an equilibrium occurring, the rate of photodegradation of phenol has no effect once exceeding this plateau value (the saturation stage). This phenomenon is possibly explained by the notion of how the photon adsorption coefficient starts to decrease radially as soon as the catalyst dose hits a specific threshold (the saturation phase). As an outcome, a high concentration of catalyst can generate a light-shielding effect, which lowers the surface area exposed to photons. Ahmad et al. [19] investigation into the impact of catalyst dose revealed that, up to a certain dosage, both performance and the rate of degradation increase.

The effect of adding more Fe-beads catalyst can be attributed to the increased surface area available for photocatalytic reactions. As the Fe-beads catalyst concentration increases, more active sites are exposed on the catalyst's surface, providing additional sites for the generation of reactive radicals such as hydroxyl radicals (•OH) and superoxide anions (O2•-) under light irradiation. These radicals are crucial for the degradation of phenol pollutants, as they interact with these contaminants, breaking down their chemical Therefore, the observed increase in degradation rates with higher Fe-beads catalyst loading can be directly linked to the enhanced production of these reactive species. More catalyst means more sites for light absorption and radical formation, leading to a higher overall degradation efficiency. However, beyond a certain concentration, the trend may level off or even decrease due to light scattering or agglomeration of Fe-beads catalyst particles, which could reduce the effective surface area and hinder efficient radical generation.

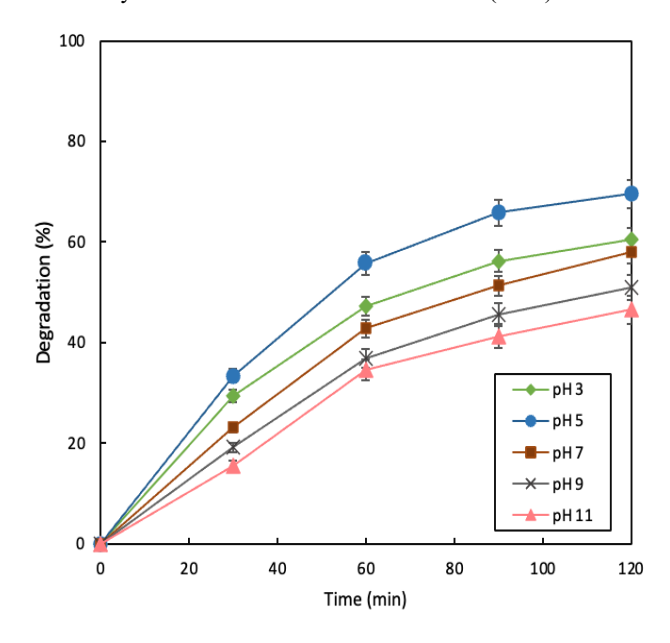


Figure 3. Effect of pH solution for Fe-beads catalyst [pH = X; W =  $2.0 \text{ g L}^{-1}$ ; C =  $20 \text{ mg L}^{-1}$ ; t = 2 h; T = 303.15 K]

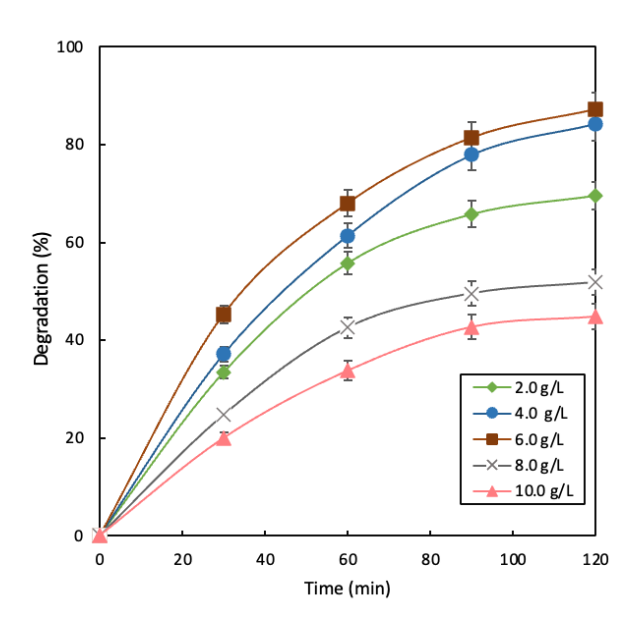


Figure 4. Effect of catalyst dosage for Fe-beads catalyst [pH = 5; W = X; C = 20 mg L<sup>-1</sup>; t = 2 h; T = 303.15 K]

According to the type, concentration, and presence of any other chemicals in the water-based material, the frequency and efficiency of a pollutant's photocatalytic destruction are regulated. The adsorption of phenol on the surface of the Fe-beads catalyst was applied to study the correlation between photocatalysis of the beads catalyst and initial concentration of pollutant. Fe-beads catalyst achieved the highest degradation percentage of 87.19% at 20 mg L<sup>-1</sup> after 2 h of irradiation (**Figure 5**). Studies show that when initial reactant

concentration rises, phenol photodegradation reduces. The primary cause of this problem is the scarcity of active sites on catalyst bead surfaces. For example, photons and aggressive reactive species find it difficult to coexist on the catalytic surface of Fe-beads catalyst when phenol concentrations are elevated. Essentially, the pollutant occupied more active sites on the bead-based catalyst when the initial reactant concentration was high, thereby reduced the rate of degradation and prevented the generation of oxidants. In this examination, the quantity of hydroxyl

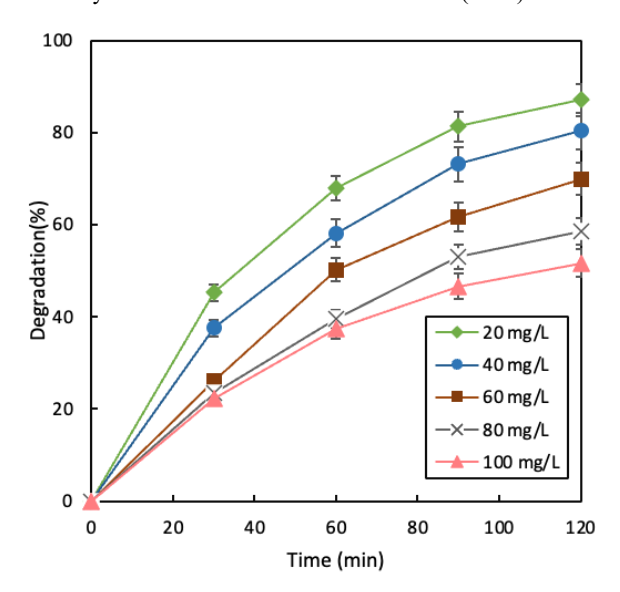


Figure 5. Effect of initial concentration for Fe-beads catalyst [pH = 5; W = 6.0 g L<sup>-1</sup>; C = X; t = 2 h; T = 303.15 K]

radicals generated in the systems remains fixed due to the fixed amount of Fe-beads catalyst and  $H_2O_2$  concentration. Hence, the minimal amount of hydroxyl radicals within the system relative to the abundant pollutants molecules was identified being the cause of a reduction in the rate of degradation following a rise in the concentration of polluting molecules. The study by Ahmad et al. [19] claimed that the degradation rate decreases as the initial concentration of contaminants increases.

From the findings, one of the most notable advantages is their magnetic separability. Unlike conventional photocatalysts, which often require centrifugation or filtration for recovery after use, Fe-beads catalyst can be easily separated from the reaction mixture using an external magnetic field. This feature significantly simplifies the recovery process, eliminates the need for complex filtration systems, and reduces catalyst loss, leading to better recyclability and longer operational life. In addition to their separability, Febeads exhibit robust structural properties that make them more suitable for repeated use in photocatalytic processes. The magnetic core of the beads provides a high degree of mechanical stability, which helps to prevent catalyst degradation over time. The findings suggested the functional groups like carboxyl or hydroxyl can increase the adsorption of phenol

pollutants, improving the overall efficiency of the photocatalytic reaction. This surface modification can also enhance the light absorption of the beads, helping to capture more light energy and promote better photocatalytic activity under visible light conditions.

#### Conclusion

The synthesised magnetic bead catalyst possesses tremendous photocatalytic capability of phenol degradation at maximum photodegradation at contact times of 2 h with the optimal conditions were achieved at pH 5 at catalyst dosage of 6.0 g L<sup>-1</sup> and an initial phenol concentration of 20 mg L<sup>-1</sup>, resulting in a phenol photodegradation efficiency of 87.29% over a two-hour duration of contact. Furthermore, this photocatalytic reaction yields safe by-products that are converted to CO<sub>2</sub> and H<sub>2</sub>O. These beads' pore size, rigidity, chemical resistance, hydrophilicity, and biocompatibility have all been markedly enhanced by The modification of transformation. photocatalyst beads increased the number of active sites, and enhanced their morphology and selectivity towards contaminants, thereby significantly boosting their photocatalytic efficiency in degrading phenol in wastewater. In overall, the current study demonstrated the application of magnetic bead catalyst may offer a fresh approach with exceptional performance pace to treating wastewater obstacles.

# Acknowledgement

The authors are grateful for the financial support by the Fundamental Research Grant Scheme (FRGS/1/2022/STG05/UNIKL/02/5) from Ministry of Higher Education Malaysia (MOHE) and the Universiti Kuala Lumpur Branch Campus Malaysian Institute of Chemical and Bioengineering Technology (UniKL MICET) for their support.

#### References

 Rashid, S., Zaid, A., Per, T. S., Nisar, B., Majeed, L. R., Rafiq, S., Wagay, N. A., Shah, N. U. D., Rather, M. A., Zulfiqar, F. and Wani, S.

- H. (2023). A critical review on phytoremediation of environmental contaminants in aquatic ecosystem. *Scienze Fisiche e Naturali*, 34: 749-766.
- 2. Liaquat, I., Munir, R., Abbasi, N. A., Sadia, B., Muneer, A., Younas, F., Sardar, M. F., Zahid, M., and Noreen, S. (2024). Exploring zeolite-based composites in adsorption and photocatalysis for toxic wastewater treatment: Preparation, mechanisms, and future perspectives. *Environmental Pollution*, 349: 123922.
- Naghan, D., Azari, A., Mirzaei, N., Velayati, A., Tapouk, F., Adabi, S., Pirsaheb, M. and Sharafi, K. (2015). Parameters effecting on photocatalytic degradation of the phenol from aqueous solutions in the presence of ZnO nanocatalyst under irradiation of UV-C light. Bulgarian Chemical Contamination, 47: 14-18.
- 4. Ahmadi, E., Kakavandi, B., Azari, A., Izanloo, H., Gharibi, H. and Mahvi, A. (2016). The performance of mesoporous magnetite zeolite nanocomposite in removing dimethyl phthalate from aquatic environments. *Desalination Water Treatment*, 57: 27768-27782.
- 5. Ingole, R. S., Lataye, D. H., and Dhorabe, P. T. (2016). Adsorption of phenol onto banana peels activated carbon. *Journal of Civil Engineering*, 21(1): 100-110.
- 6. Pulli, E., Rozzi, E. and Bella, F. (2020). Transparent photovoltaic technologies: Current trends towards upscaling. *Energy Conversation Management*, 219: 112982.
- 7. Hanafi, M. F. and Sapawe, N. (2020) Electrosynthesis of zirconia nanoparticle catalyst with enhanced photodegradation of methyl orange. *Test Engineering and Management*, 83: 13610-13615.
- 8. Hanafi, M. F. and Sapawe, N. (2020) Photodegradation of remazol brilliant blue dye using zirconia nanoparticle catalyst. *Test Engineering and Management*, 83: 13667-13672.
- 9. Hanafi, M. F., Harun, N. F. C., Sapawe, N. and Raidin, A. (2020). Electrobiosyntesis of NiO using rambutan leaves for photodegradation of remazol brilliant blue dye. *Malaysian Journal of Analytical Sciences*, 24(2): 227-235.
- Hanafi, M. F., Mustafa, A. N. and Sapawe, N. (2020) Electrosynthesis of silver oxide deposited onto hotspring mud with enhanced

- degradation of Congo red. *Malaysian Journal of Analytical Sciences*, 24(2), 266-275.
- 11. Khairol, N. F., Sapawe, N. and Danish M. (2020). Tailoring the optical properties of zinc/copper–incorporated onto eggshell synthesized via electrochemical method. *Materials Today: Proceeding*, 31(1): 241-244.
- 12. Deng, Y. and Zhao, R. (2015). Advance oxidation processes (AOPs) in wastewater treatment. *Current Pollution Reports*, 1: 167-176.
- 13. Hanafi, M. F. and Sapawe, N. (2020)
  Performance of nickel catalyst toward photocatalytic degradation of methyl orange.

  Materials Today: Proceedings, 31(1): 257-259.
- 14. Choi, K. H., Park, S. Y., Park, B. J., and Jung, J. S. (2017). Recyclable Ag-coated Fe<sub>3</sub>O<sub>4</sub>@TiO<sub>2</sub> for efficient photocatalytic oxidation of chlorophenol. Surface and Coatings Technology, 320: 240-245.
- 15. Zhu, Y., Zhang, L., Gao, C. and Cao, L. (2000). The synthesis of nanosized TiO<sub>2</sub> powder using a sol-gel method with TiCl<sub>4</sub> as a precursor. *Journal of Materials Science*, 35: 4049-4054.
- 16. Huang, K., Lv, Y., Zhang, W. and Sun, S. (2015). One-step synthesis of Ag<sub>3</sub>PO<sub>4</sub>/Ag photocatalyst with visible-light photocatalytic activity. *Journal of Materials Research*, 18: 939-945.
- 17. Wan, S., Zhao, W., Xiong, D., Li, S., Ye, Y., and Du, L. (2022). Novel alginate immobilized TiO<sub>2</sub> reusable functional hydrogel beads with high photocatalytic removal of dye pollutions. *Journal of Polymer Engineering*, 42(10).
- 18. Tran N. B. T., Duong, N. B. and Le, N. L. (2021). Synthesis and characterization of magnetic Fe<sub>3</sub>O<sub>4</sub>/Zeolite NaA nanocomposite for the adsorption removal of methylene blue potential in wastewater treatment. *Journal of Chemistry*, 14.
- 19. Ahmad, I. (2020). Comparative study of metal (Al, Mg, Ni, Cu and Ag) doped ZnO/g-C<sub>3</sub>N<sub>4</sub> composites: Efficient photocatalysts for the degradation of organic pollutants. *Separation and Purification Technology*, 251: 117372.
- 20. Shi, X., Tian, A., You, J., Yang, H., Wang, Y. and Xue, X. (2018). Degradation of organic dyes by a new heterogeneous Fenton reagent-Fe<sub>2</sub>GeS<sub>4</sub> nanoparticle. *Journal of Hazardous Materials*, 353: 182-189.